

## **Plasma jets produced in a single laser beam interaction with a planar target**

Ph. Nicolai<sup>1</sup>, V.T. Tikhonchuk<sup>1</sup>, A. Kasperczuk<sup>2</sup>, T. Pisarczyk<sup>2</sup>,  
S. Borodziuk<sup>2</sup>, K. Rohlena<sup>3</sup>, J. Ullschmied<sup>4</sup>

<sup>1</sup> *Centre Lasers Intenses et Applications, Université Bordeaux 1, 33405 Talence, France*

<sup>2</sup> *Institute of Plasma Physics and Laser Microfusion, 00-908 Warsaw, Poland*

<sup>3</sup> *Institute of Physics AS CR, 182 21 Prague 8, Czech Republic*

<sup>4</sup> *Institute of Plasma Physics AS CR, 182 00 Prague 8, Czech Republic*

The formation, propagation and stability of plasma jets are fundamental issues in the astrophysical context and for the Inertial Confinement Fusion. Previous experiments demonstrated a possibility of jet creation by using specially designed conically shaped targets and high energy lasers such as NOVA, GEKKO-XII and NEL [1]. We are reporting here on the jet generation in a more simple geometry by using a large focus laser-plasma interaction at the Prague Asterix iodine Laser System (PALS) [2]. Pulses of 0.4 ns duration at a 100 – 200 J level at the first and third harmonics (1.35 and 0.44  $\mu\text{m}$ ) were focused on massive planar metallic targets at the spot radius varying from 35 to 500  $\mu\text{m}$  (the focal point was located inside the target). We investigated an influence of the focusing conditions, laser wavelength, and the target atomic number on the plasma jet formation. The information about geometry of plasma expansion, plasma dynamics and electron density distributions were obtained by means of a three-frame laser interferometric system [3]. The temporal resolution of the interferometer, 0.3 ns, was determined by the diagnostic pulse duration. The spatial resolution of 20  $\mu\text{m}$  was deduced from the target edge washers. The delay between subsequent frames was set to 3 ns.

A typical sequence of electron density distributions is presented in Fig. 1. For all three materials, aluminium, copper and silver, a plasma jet is present and it remains visible during a long time. Distinctly, the jet becomes narrower as the atomic number increases. This observation indicates an important role of radiative processes. The last sequence shows the effect of a laser focal spot radius and a laser wavelength. A transition to shorter wavelength and larger spot radius improves the jet. For small radii, but keeping the laser energy constant, the ablated plasma ejection is quasi-isotropic, whereas, as the spot radius increases, the plasma extends along the laser axis. The optimum conditions for the PALS laser system correspond to the spot radius of 300  $\mu\text{m}$ . Considering the contour line corresponding to the electron density of  $10^{18} \text{ cm}^{-3}$ , we estimate the jet length of 2 mm, the jet diameter of 0.4 mm for heavy target materials, the maximum axial jet velocity of 700 km/s, and the jet life time more than 17 ns.

The simulations of the plasma dynamics were performed with the laser-plasma interaction hydrodynamic code FCI2 [4]. It has been compared with other similar codes as LASNEX and it successfully reproduced previous experiments [5] with similar irradiation conditions. The code includes two-dimensional hydrodynamics, ion and classical or nonlocal electron conduction, thermal coupling and detailed radiation transport. Ionization, equations of state and opacity data are tabulated, assuming a local thermodynamic equilibrium (LTE) or a non-LTE depending on the plasma parameters. The laser propagation, refraction and collisional absorption are treated by a ray tracing algorithm. A resistive MHD package accounting for the azimuthal magnetic fields was also included.

In order to identify the physical origin of the jet formation, certain physical effects were artificially switched on or off. The reference simulation was carried out under the following conditions: the laser energy 100 J, the pulse duration  $\tau = 0.4$  ns with the temporal shape  $I(t) \propto \sin^2(t/\tau)$ . For the spot radius  $R_L = 300 \mu\text{m}$ , the maximum laser intensity was  $8.8 \times 10^{13} \text{ W/cm}^2$ . The intensity profile on the target has a super-Gaussian distribution,  $I(r) \propto \exp[-(r/R_L)^n]$ . It was verified in simulations the effect of jet formation is robust and its shape can be controlled by changing the power  $n$  in the laser intensity distribution.

The laser beam with  $n = 8$  was focused on a massive copper solid target. The flux limiter for the electron heat conduction was set to equal to 8%, and we performed several runs where certain physical effects were artificially switched off. Figure 2-a presents iso-densities, at 5 ns, well after the end of the laser pulse. This simulation without the radiation transport obviously does not reproduce the experimental result. The plasma flow is too broad. This result has to be

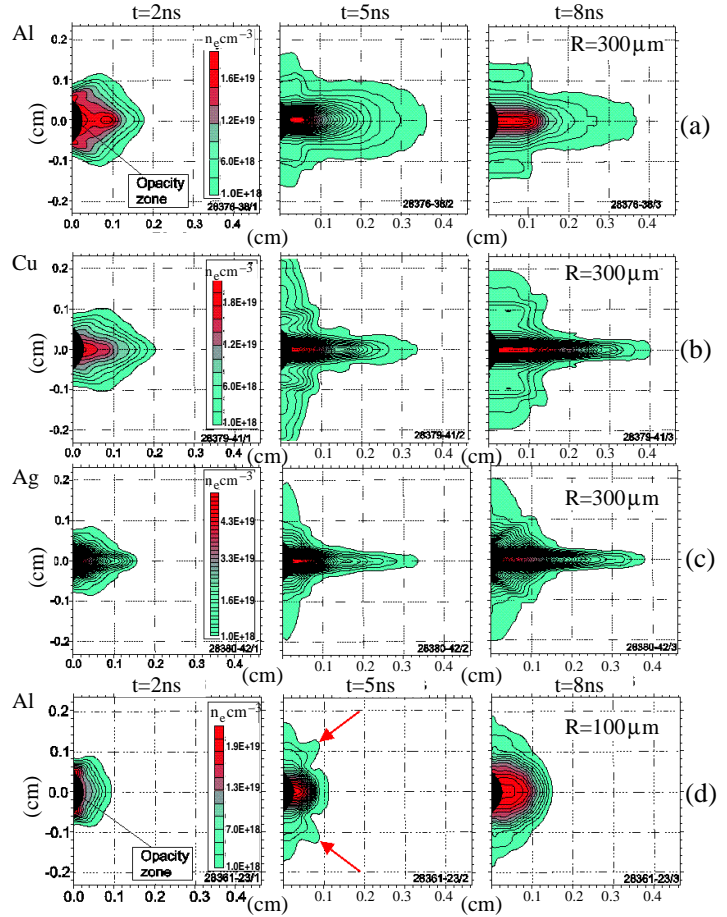


Figure 1: Experimental sequence of the electron density isolines at 2, 5, 8 ns for  $R_L = 300 \mu\text{m}$ ,  $E_L = 100 \text{ J}$  and the wavelength of  $0.438 \mu\text{m}$  for Al (a), Cu (b) and Ag (c) targets; (d) for  $R_L = 100 \mu\text{m}$  and Al target

compared with those shown in Fig. 2-b. In this simulation, the radiation transport is turned on. The results are much closer to the experiment. Initially spherical, the plasma plume is elongated after a few ns. Its radius is two-three times smaller than in the previous case and the height is about 3 mm is also in agreement with the experiment. Due to the radiative cooling, the plasma temperature decreases 2.5 times to the value around 50 eV. Comparing both simulations, we can see that the radiation cooling reduces the pressure by a factor 30. Consequently, the characteristic expansion velocities are smaller with the radiation transport (545 km/s at the jet tip) than without (600 km/s), specifically for the radial expansion (180 km/s compared with 270 km/s).

The magnetic field generation and the nonlocal heat conduction are the competing processes that may operate under the present conditions and could be partly responsible of the jet formation. The magnetic field reaches a maximum of 1 MG, during the pulse duration and then it decreases quickly after the pulse end. At  $t = 5$  ns it is only 8.6 kG and its effect on the plasma motion is completely negligible (Fig. 2-c). In order to address the effect of a tighter laser focusing, for the same energy and pulse duration, the focal spot size was reduced three times, so the laser intensity was nine times higher. The smaller energy deposition volume leads to a higher temperature, a smaller absorption and a higher plasma pressure. The expansion for a smaller focal spot size is faster and the plasma takes a spherical shape (Fig. 2-d). The density falls below the resolution limit of a few  $10^{17} \text{ cm}^{-3}$  at the distance less than 1 mm.

The laser energy distribution in the focal spot has an impact on the jet formation. For comparison, we present in Fig. 2-e, the density profile obtained using a gaussian shape,  $n = 2$ . The jet still appears, but an energy distribution change modifies the form of the jet. In order to test the target atomic number dependance, we replaced copper by aluminium in the simulation. As expected, one can see in Fig. 2-f that the jet becomes wider and more isotropic which is consistent

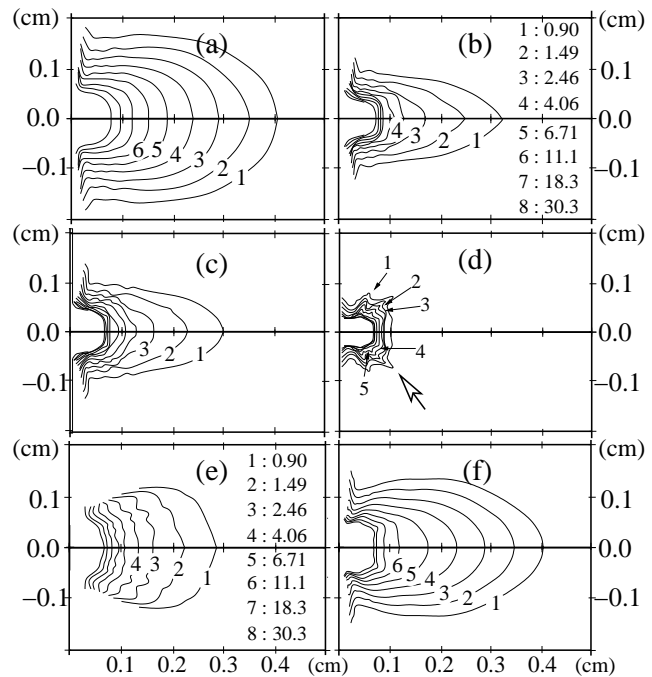


Figure 2: Electron density distributions at  $t = 5$  ns, for  $E_L = 100$  J,  $\tau_L \sim 400$  ps,  $\lambda_L \sim 0.438 \mu\text{m}$  and  $R_L = 300 \mu\text{m}$ . Without the radiation transport (a), with the radiation transport (b), with the magnetic fields (c), with a smaller laser spot radius (d), with a different energy distribution the the focal spot (e) and with an aluminium target (f). The densities are in  $10^{18} \text{ cm}^{-3}$ .

with a less efficient radiation cooling.

The computational results can be confirmed from a dimensional analysis. The characteristic hydrodynamic time depends on the focal spot radius  $R_L$  and on the ion acoustic velocity  $c_s$ :  $t_h = R_L/c_s = 0.1 R_L (A/Z)^{1/2} T^{-1/2}$  ns, where  $A$  and  $Z$  are the atomic mass in units of proton mass and the ion charge,  $R_L$  is in  $\mu\text{m}$  and  $T$  in eV. The radiative cooling time is the ratio of the plasma thermal energy and radiated power. For simplicity here we neglect the line emission and account only for the bremsstrahlung emission [6]:  $P_{br} = 1.7 \times 10^{-32} Z n_e^2 T^{1/2} \text{ W/cm}^3$ , where the electron plasma density is in  $\text{cm}^{-3}$ . It has to be chosen in the region of maximum radiation losses, that is, between the critical density and the ablation front. The plasma energy density is defined as  $E_p = 1.5 n_e T = 2.4 \times 10^{-19} n_e T \text{ J/cm}^3$ . Consequently, the radiation cooling time reads:  $t_r = E_p/P_{br} = 1.4 \times 10^{22} T^{1/2}/Z n_e$  ns. Then, for the typical parameters of this experiment:  $R_L = 300 \mu\text{m}$ ,  $A = 63$ ,  $Z = 15$ ,  $T = 100 \text{ eV}$ , and  $n_e = 10^{22} \text{ cm}^{-3}$ , we find the hydrodynamic time  $\sim 6$  ns and the radiation time  $\sim 0.9$  ns. The radiative cooling makes an important effect in agreement with the observations and the simulations. In the contrary, for the tighter focusing  $R_L = 100 \mu\text{m}$ , the temperature is higher  $T \sim 300 \text{ eV}$  ( $Z = 20$ ) and consequently the hydrodynamic time is shorter  $\sim 1$  ns, while the radiation time becomes longer  $\sim 1.2$  ns. In that case the radiative losses are less important and the plasma expansion is more symmetric.

In conclusion, we have studied the formation of a plasma jet using a single laser beam and a simple planar massive target. The experiment and the simulations indicate that this jet may be launched using a relatively low laser energy. Under these conditions, the dissipative processes can be neglected and the laser produced jet can be scaled to astrophysical conditions. Moreover, such a jet is rather flexible and could be used for modeling of interaction between the astrophysical jet and the ambient clouds. For that, one place in front of the jet, a solid foil, a foam or a gas jet, by changing the angle of the laser beam incidence by a few tens of degrees. In addition, by modifying the pulse duration and intensity, one can modify the velocity and the density of the jet. Always using a single laser beam, one could build a series of pulses with an increasing intensity. Each pulse induces a jet faster than the previous one. A correct timing of such a pulse sequence should create a series of plasma jets interacting one with another.

## References

- [1] B. E. Blue, S. V. Weber, S. G. Glendinning *et al.*, Phys. Rev. Lett. **94**, 095005 (2005)
- [2] K. Jungwirth, A. Cejnarova, L. Juha *et al.*, Phys. Plasmas **8**, 2495 (2001)
- [3] S. Borodziuk, N. Demczenko, S. Gus'kov *et al.*, Opt. Appl. **35**, 242 (2005)
- [4] E. Buresi, J. Coutant, R. Dautray *et al.*, Laser Part. Beams **4**, 531 (1986)
- [5] Ph. Nicolai, M. Vandenboomgaerde, B. Canaud *et al.*, Phys. Plasmas **7**, 4250 (2000)
- [6] D. L. Book, *NRL Plasma Formulary*, (Washington D.C., NRL) p. 52 (1980)